EVOLUTION & DEVELOPMENT 16:4, 224–232 (2014)
DOI: 10.1111/ede.12085

Developmental integration in a functional unit: deciphering processes from adult dental morphology

Gaëlle Labonne,[a,b,*] Nicolas Navarro,[a,b] Rémi Laffont,[b] Carmela Chateau-Smith,[c] and Sophie Montuire[a,b]

[a] Laboratoire PALEVO, Ecole Pratique des Hautes Etudes, 6 bd Gabriel, Dijon, France
[b] UMR uB/CNRS 6282-Biogéosciences, Université de Bourgogne, 6 bd Gabriel, Dijon, France
[c] UFR SVTE Université de Bourgogne, 6 bd Gabriel, Dijon, France
*Author for correspondence (e-mail: gaelle.labonne@u-bourgogne.fr)

SUMMARY The evolution of mammalian dentition is constrained by functional necessity and by the non-independence of morphological structures. Efficient chewing implies coherent tooth coordination from development to motion, involving covariation patterns (integration) within dental parts. Using geometric morphometrics, we investigate the modular organization of the highly derived vole dentition. Integration patterns between and within the upper and lower molar rows are analyzed to identify potential modules and their origins (functional and developmental). Results support an integrated adult dentition pattern for both developmental and functional aspects. The integration patterns between opposing molar pairs suggest a transient role for the second upper and lower molars during the chewing motion. Upper and lower molar rows form coherent units but the relative integration of molar pairs is in contradiction with existing developmental models. Emphasis on the first three cusps to grow leads to a very different integration pattern, which would be congruent with developmental models. The early developmental architecture of traits is masked by later stages of growth, but may still be deciphered from the adult phenotype, if careful attention is paid to relevant features.

INTRODUCTION

The primitive dentition of tetrapods is composed of numerous conical teeth, which are similar between and within lower and upper dental rows (Reisz 2006). Absent from primitive dentition, occlusion was acquired several independent times during the evolutionary history of synapsids (Reisz 2006). Occlusion involved profound morphological modifications of teeth, probably an adaptive convergence to a specific diet (Reisz 2006; Evans et al. 2007). Evolution toward exact occlusion leads to an increase in dental complexity, especially the addition of cusps (Luo et al. 2001; Kielan-Jaworowska 2004; Jernvall and Thesleff 2012). Great variability of heterodonty along the jaw is characteristic of mammalian dentition and is considered to be linked to diet (Evans et al. 2007). These innovations in tooth morphology are presumed to contribute to the evolutionary success of mammals (Jernvall and Thesleff 2012).

Tooth morphogenesis and related molecular processes are better understood through advances in developmental biology (Jernvall and Thesleff 2000; Kavanagh et al. 2007). Mammalian tooth initiation reiteratively uses the same signaling cascade from the determination of tooth region to the location of cusps on the individualized teeth (Jernvall and Thesleff 2000). The primary enamel knot provides tooth crown location; molar development is sequential from the anterior to the posterior parts of the row (Jernvall and Thesleff 2000, 2012). The size of the anterior molars affects the size of the posterior molars because of the dynamic balance between intermolar inhibition and mesenchymal activation (Kavanagh et al. 2007). This inhibitory cascade model occurs during the very early stages of molar development when the secondary enamel knots are formed (Kavanagh et al. 2007; Charles et al. 2009). The number of these enamel knots determines the molar cusp pattern and thus the shape of the tooth crown (Jernvall and Thesleff 2000, 2012; Catón and Tucker 2009).

The evolution of dental morphology is constrained by functional necessity (Reisz 2006; Polly 2012; Smits and Evans 2012). Efficient chewing implies consistent tooth coordination from development to motion, so the morphological modification of one tooth implies changes in the other teeth. Covariations may occur because of this coordination between parts of the dentition. Morphological integration (Olson and Miller 1958) is usually studied from covariation patterns within organisms in order to identify potential modules and processes (e.g., function and development) responsible for such organization. Modules can be defined as units within which strong covariations (integration) are observed, while covariations between such units are weak (Wagner 1996; Klingenberg 2004). Integration and modularity can be studied at different levels of organization (Eble 2005) and in various non-exclusive

contexts, such as function and development (Breuker et al. 2006). A morphometric framework has been proposed to infer the factors responsible for the integration patterns observed in adult morphology (Klingenberg 2004, 2008). Fluctuating asymmetry (FA) is commonly defined as random deviations from perfect bilateral symmetry, resulting from small developmental perturbations (Palmer and Strobeck 1986). Trait covariation in FA arises from direct developmental interactions because of common signaling or shared developmental pathways. Thus, FA may be used to assess developmental integration. Trait covariation in among-individual variation (IndVar) arises from direct developmental interactions and parallel variation (such as environment, genetic variation, or function). The functional aspect of dentition is therefore expressed within IndVar.

To explore patterns and processes at both developmental and functional levels, dental innovation in arvicoline rodents is a case of interest (e.g., Salazar-Ciudad and Jernvall 2002; Polly 2007). During their Pliocene evolutionary radiation, arvicolines acquired a highly derived molar phenotype (Chaline et al. 1999). Molars are high crowned and hypselodont, with a complex occlusal surface composed of alternate cusps (Fig. S1). The occlusal surface of arvicoline molars is flat in comparison with that of most mammals. The number of cusps varies, both for the teeth on a row and between the upper and lower molar rows, producing a particular form of occlusion between opposing molars. Molar proportions in voles are exceptional among rodents, with a highly elongated first lower molar (Renvoisé et al. 2009; Labonne et al. 2012). The developmental quasi-independence of lower molars and the morphological integration of the row have been demonstrated for *Microtus arvalis* (Laffont et al. 2009). The ancestral tribosphenic molar had fewer cusps than the vole molar. The mouse (*Mus musculus*), the model organism for mammalian developmental studies, also has fewer molar cusps than the vole. Despite this highly derived tooth pattern in voles, the first three cusps to grow on upper and lower molars have been homologized for rodents (Stehlin and Schaub 1951; Van der Meulen 1973; Marivaux et al. 2004). These cusps are called protocone, paracone, and metacone on upper molars, and protoconid, metaconid, and entoconid on lower molars (Fig. S1; Hershkovitz 1967; Van der Meulen 1973).

The aim of this work is to investigate the specific dental phenotype and occlusion for voles, using geometric morphometrics. Analyzing among-individual variation and FA, we will test if vole dentition reflects developmental and functional integration of traits. Three aspects will be assessed: Does the adult dentition express some cohesion for both developmental and functional aspects? What is the morphological and developmental organization within the dental row? Using current knowledge on odontogenesis, how relevant is the use of the adult phenotype to infer the integration pattern for the early stages of development?

MATERIALS AND METHODS

Sample and landmark digitizing

We used the genus *Microtus*, typically used as models in odontogenesis studies, to investigate the derived dental phenotype of voles. The study sample was composed of 182 wild-trapped *M. arvalis* from France (Espezel, $n = 48$; Versailles, $n = 36$; Parc de la Vanoise, $n = 34$; Vittel, $n = 32$; and St Michel en l'Herm, $n = 32$). Cleaned skulls were obtained from the collection of the CBGP (INRA, Montpellier, France).

Molar orientation was standardized on the lower row, following Brunet-Lecomte (1988) and adapted here for the upper row. Forty-seven 2D landmarks were defined on lower molars (22 landmarks on m1, 12 on m2, and 13 on m3) and 38 landmarks on upper molars (13 landmarks on M1, 10 on M2, and 15 on M3). Most of these landmarks correspond to maximal curvature points of salient and re-entrant triangles and loop tips (Fig. S1). One person (G.L.) digitized all the landmarks, using a Nikon MM-60 measuring microscope (Nikon-Japan, Tokyo, Japan). Left and right sides of all individuals were processed twice to assess measurement error. From this setup, a simplified landmark scheme was derived to focus on the first three cusps to occur during development (protocone, paracone, and metacone on upper molars, and protoconid, metaconid, and entoconid on lower molars, Fig. S1).

Geometric morphometrics

Molar rows were superimposed using a full generalized Procrustes analysis with matching symmetry (Dryden and Mardia 1998; Klingenberg and McIntyre 1998). The full tangent coordinates obtained from this analysis (Dryden and Mardia 1998) were then used in the study. For analyses within rows, we followed the simultaneous-fit approach of Klingenberg (2009), where the Procrustes superimposition is performed on the whole dental row, and not separately for each molar (separate-fit approach). Shape corresponds to all geometric information that is not size, position or orientation of the object. This approach incorporates simultaneous covariation of the different parts composing the object. Thus the shared covariation originating from the relative position, orientation and size of molars within the dental row is genuine shape variation at the level of the whole row. The separate-fit approach was used in complement to the simultaneous-fit approach for comparison with previous studies, and for analyses between rows. The variability of molar shapes was estimated using the multivariate generalization of the coefficient of variation (CV_p), which is independent to the number of variables (Van Valen 1974, 2005). This coefficient was computed according to: $CVp = 100\times \sqrt{\sum S_j^2 / \sum \mu_j^2}$, where S_j^2 and μ_j^2 are, respectively, the variance and mean of the jth coordinates for a given molar (Van Valen 2005).

Quantifying morphological and developmental integration

Morphological integration was estimated on IndVar and developmental integration on FA. IndVar corresponds to the variation in the left–right averages of individuals. FA was computed from the left–right differences between tangent coordinates, corrected for mean asymmetry. The main covariation patterns among subsets of landmarks in molars were visualized using a three-block partial least squares analysis (3B-PLS) for each row (Bookstein et al. 2003). The algorithm used (Bookstein et al. 2003) generalizes the classical algorithm based on matrix multiplication for two-block PLS (Streissguth et al. 1993). The PLS method is used to illustrate all the patterns of covariation among the three molars of a row, thus representing the maximum of shared covariance.

Covariation between teeth and rows was quantified using the *Rv* coefficient (Escoufier 1973), a multivariate generalization of the squared Pearson coefficient (Escoufier 1973; Klingenberg 2009) that generalizes the second 2B-PLS summary statistics of Rohlf and Corti (2000): the amount of cross-covariance between sets was normalized by its maximal possible value (Laffont et al. 2009). The *Rv* coefficient of 0 indicates completely uncorrelated subsets of landmarks, corresponding to independent modules. The value of 1 corresponds to a subset that differs only by any combination of rotation translation and scaling, indicating that the subsets are fully integrated (Klingenberg 2009). The null-hypothesis of complete modularity ($Rv = 0$) was assessed using 10,000 permutations of subsets across individuals (Klingenberg 2009). A Procrustes fit follows the permutation when the simultaneous-fit approach is used. This approach corrects the shared covariances imposed by the simultaneous fit, which can artificially inflate *Rv* coefficients between subsets.

The analysis is performed on complete and reduced landmark schemes. The hypothesis, suggested by the developmental model, is that adjacent molars are more correlated than more distant molars (Kavanagh et al. 2007). On the complete scheme, the analysis is performed on both FA and IndVar. The reduced landmark scheme corresponds to the first three cusps to grow on each molar. The aim of this scheme is to test on FA whether early developmental integration may be inferred from the adult phenotype, by considering only the structures developing precociously on molars.

The contribution of molar relative size, orientation, and position to the row covariation signal was explored to highlight the differences between simultaneous and separate-fit approaches. Isolated or joint influence of these different sources on the pattern of covariation may be apprehended using their individual and consensus estimates. Such estimates were used to transform molar shape spaces to the shape space of the molar row: estimations of the factors of interest were added to the molar shapes obtained from separate Procrustes fits, while keeping other factors invariant. The consensus estimates were used to set one or more factors as constants, while variable factors were based on individual estimates. Variance–covariance (VCV) matrices were then computed and compared to discover to what extent the factors tested influenced covariation. Analyses were performed with Matlab® version 6.5 and R version 2.15.3 (R Development Core Team 2011).

RESULTS

Preliminary results

The presence of gross outliers was tested sequentially using Mahalanobis distances, and 13 outliers were detected and removed, leaving 169 individuals in the dataset. Size and geographical origin of populations as well as their interaction may be a pervasive source of noise in the analysis of morphological variation (e.g., Renvoisé et al. 2012) and in analyses of modularity and integration (e.g., Mitteroecker and Bookstein 2007; Klingenberg 2013). A multivariate analysis of covariance (MANCOVA) was computed for each level at which modularity analysis would later be assessed (Table S1). All these results indicate the influence of size and population and their interaction on shape: these effects were corrected in the subsequent analyses.

Coefficients of variation of the six molars are relatively low (from 4% to 7%). The most variable tooth in the lower row is m3 ($CV_p = 4.14\%$ for m1, $CV_p = 4.91\%$ for m2, and $CV_p = 5.65\%$ for m3). On the upper row, M2 is the most variable molar ($CV_p = 4.00\%$ for M1, $CV_p = 6.98\%$ for M2, and $CV_p = 6.05\%$ for M3).

The morphometric framework for quantifying developmental integration is based on the covariation of FA. The amount of FA that must be significant relative to errors in positioning and digitizing was confirmed by Procrustes ANOVA (Table S2) (Klingenberg and McIntyre 1998).

Integration among molars within the dental row

The three molar pairs are integrated at both IndVar and FA levels within the upper and lower rows (Table 1). Relative integration among molar pairs for IndVar and for FA show similar results, with the most integrated pair being M1–M2 on the upper row, while on the lower row m2–m3 is the most integrated pair.

Within-row integrations among molars with separate fit are weaker than the ones with simultaneous fit (Table 2). For FA, the *Rv* coefficients are similar for the three molar pairs in each row, but the only two pairs to be integrated are M1–M2 and M1–M3.

On the upper row (Fig. 1A), the PLS visualization of IndVar shows that molars tend to covary toward the same side (lingual), except for the anterior part of M3. For FA, M2 rotates toward the buccal side in association with relative stability for the other teeth. On the lower row (Fig. 1B), for both FA and IndVar, m2 moves to the buccal side, while a great lingual rotation of m3 is observed.

Table 1. *Rv* coefficients and *P*-values on the complete landmark scheme after simultaneous fit

	Variation among individuals		Fluctuating asymmetry	
	Rv	*P*	*Rv*	*P*
Row to row	0.08	0.00	0.07	0.03
M1–M2	0.49	0.00	0.40	0.00
M1–M3	0.37	0.00	0.30	0.00
M2–M3	0.30	0.00	0.23	0.00
m1–m2	0.29	0.00	0.26	0.00
m1–m3	0.32	0.00	0.32	0.00
m2–m3	0.49	0.00	0.49	0.00
M1–m1	0.08	0.00	0.05	0.47
M2–m2	0.03	0.20	0.03	0.21
M3–m3	0.05	0.03	0.05	0.02
M1–m2	0.05	0.05	0.05	0.03
M1–m3	0.06	0.01	0.03	0.30
M2–m1	0.05	0.06	0.03	0.53
M2–m3	0.04	0.05	0.03	0.21
M3–m1	0.07	0.01	0.04	0.32
M3–m2	0.05	0.02	0.06	0.00

Integration between upper and lower rows

The integration of the rows (Table 1) is weak but significant for IndVar and for FA. Pairs of opposing molars, M1–m1 and M3–m3, are weakly but significantly integrated for IndVar, whereas M2–m2 are two independent modules. All the other molar pairs are integrated for IndVar, except m1–M2. For FA, M3–m3 is the only integrated pair of opposing molars; few of the non-opposing molar pairs are integrated (M1–m2 and M3–m2).

Identifying influential factors of covariation in Procrustes superimposition

The addition of relative sizes of molars to shape affects the pattern of covariation only slightly (Figs. 2 and S2). For example, the VCV matrix for separate fit closely resembles the VCV matrix obtained by the addition of relative sizes to the separate fit, indicated here by similar shades of blue (Fig. 2). The joint influences of relative orientation and position on shape involve covariations similar to those observed with a simultaneous fit. Position is the main factor inducing a high correlation between M1 and M2 and between m2 and m3 (dark surfaces). In contrast, covariation between the first and third molars is mainly related to size and orientation.

Table 2. *Rv* coefficients and *P*-values on the complete landmark scheme after separate fit

	Variation among individuals		Fluctuating asymmetry	
	Rv	*P*	*Rv*	*P*
M1–M2	0.12	0.00	0.05	0.01
M1–M3	0.11	0.00	0.10	0.00
M2–M3	0.07	0.00	0.04	0.24
m1–m2	0.17	0.00	0.06	0.23
m1–m3	0.16	0.00	0.08	0.49
m2–m3	0.18	0.00	0.04	0.60

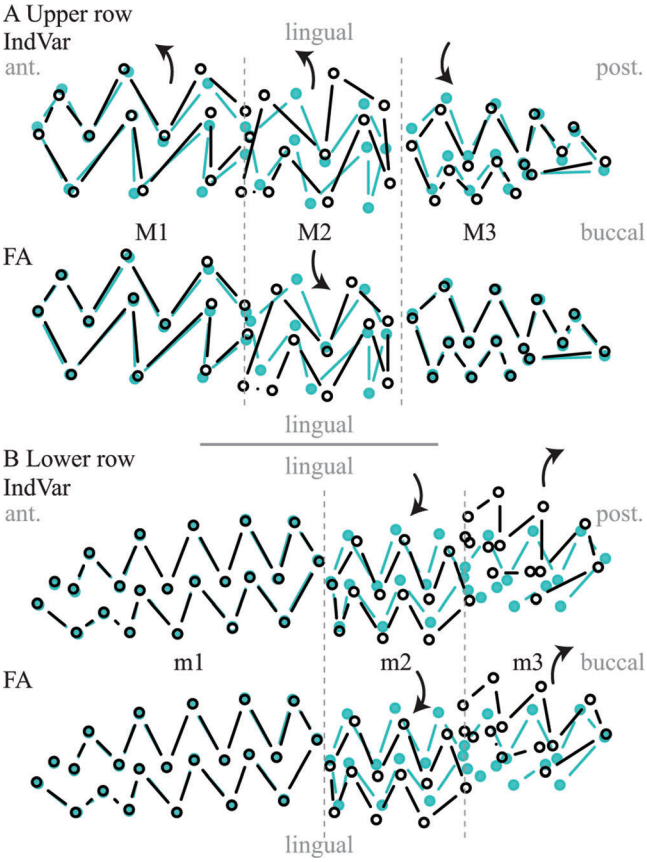

Fig. 1. Effects on the first triplet of 3B-partial-least squares (PLS) for upper row (A) and lower row (B) for both IndVar and FA. Positive effect (empty circles) is compared to the mean individual (full circles); the arrows indicate the global rotation direction of the molars between the positive effect and the mean individual. The separation of the three molars is symbolized by dotted lines.

Analyzing primitive cusps to decipher early stages of developmental integration

Integration patterns obtained from analyses based on only three cusps are more congruent with existing developmental models. All FA integrations among molars within each row are significant (Table 3). The most integrated molar pair on the upper row is M2–M3, followed by M1–M2. The most integrated pair on the lower row is m1–m2, followed by m2–m3.

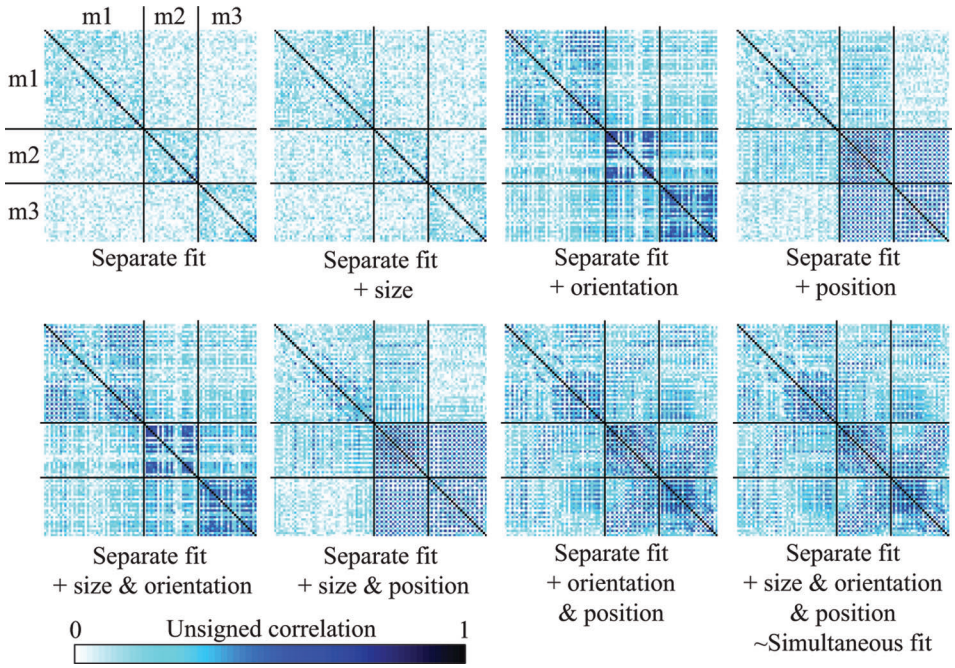

Fig. 2. A variance–covariance matrices among and within lower molars. The first (upper left) represents the separate fit and the last (lower right) is the simultaneous fit. The six others represent the analysis where one or two influential factors (size, orientation and position) are maintained constant. The variable factors are used as labels for the analyses. For example, the box labeled Separate fit + size corresponds to the VCV matrix of FA from an analysis where the only variables are the relative size and the shape from the separate fit, while the effects of relative orientation and position are constants. The VCV matrices are scaled by variances and negative values were converted to positive values, for purposes of illustration. For IndVar results, and for all results for the upper row, see supplementary material (Fig. S2).

DISCUSSION

Integration between upper and lower rows and functional interpretation

The entire molar dentition can be considered as a single unit, with development and function producing integration between upper and lower molar rows. Proper characterization of functional covariation between rows should integrate malocclusion, for example, and the approach used should quantify the relative orientation and position of the rows. But jaw movements during chewing make this approach difficult if not impossible. We therefore performed two Procrustes fits, one on upper rows and one on lower rows. Nevertheless, significant developmental and functional integration is observed at the scale of the entire molar dentition. Recent studies suggest that the mandibular movement during mastication mainly contributes to covariation between opposing tooth rows (Polly 2012; Smits and Evans 2012). Arvicoline and murine rodents have a propalinal (antero-posterior) chewing motion (Vorontsov 1979; Satoh 1997; Charles et al. 2007). For the murine *Apodemus sylvaticus*, the main shape covariation occurs between the three pairs of opposing molars, but only between M1–m1 and M2–m2 for the murine *M. musculus* (Renaud et al. 2009). For the arvicoline *M. arvalis*, M1–m1 and M3–m3 molars seem necessary for occlusion, but the M2–m2 molars are uncorrelated (Fig. 3A). The covariation pattern between opposing molars for murines (Renaud et al. 2009) contrasts with our results for voles. The reason could well involve a different propalinal movement of the jaw, resulting from the specific morphology of vole dentition. Because of bunodont molars, the murine dentition is a "key-lock" system, where upper and lower molars fit together. In contrast, the occlusal surface of the vole molar row is often considered as flat, yet in reality the upper row is slightly convex, while the lower row is concave. The absence of a "key-lock" system implies more freedom for cusps to change, and so

Table 3. *Rv* coefficients and *P*-values on the reduced landmark scheme, using the first three cusps to grow

	Fluctuating asymmetry	
	Rv	*P*
M1–M2	0.33	0.00
M1–M3	0.31	0.00
M2–M3	0.49	0.00
m1–m2	0.59	0.00
m1–m3	0.37	0.00
m2–m3	0.51	0.00

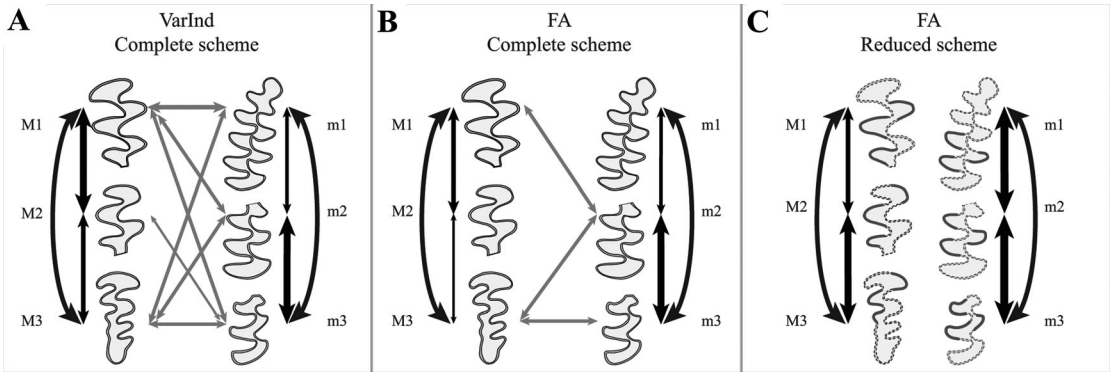

Fig. 3. Modular organization of *Microtus arvalis* dentition using the *Rv* coefficient. Modularity of upper and lower rows is tested using the complete scheme on IndVar (A) and on FA (B) and using the first three cusps to grow (C). The thickness of arrows indicates the importance of integration between molars within the row (black), and between molars in different rows (gray). Only significant *Rv*-values are plotted.

relaxation of the functional requirement is possible. The coordination between the molars at the ends of each row is necessary for efficient chewing, and the role of the second molars is more transient during motion.

Integration among molars within the dental row and developmental inferences

At the intrarow level, we used a simultaneous-fit approach on our dataset, whereas a separate-fit approach was favored in a previous study on the lower molar row of *M. arvalis* (Laffont et al. 2009). The higher *Rv*-values found here are an expected result (Klingenberg 2009) that has both biological and mathematical foundations. Using a separate-fit approach on our dataset (Table 2) achieves very similar results to those of Laffont et al. (2009): the three lower molars are developmentally independent modules and present quasi-equal morphological integration. These results are not congruent with the simultaneous-fit approach. Using separate or simultaneous fits is a matter of debate (Klingenberg 2009). The simultaneous-fit approach provides additional clues about integration, and may reveal genuine covariations that were previously masked in the separate-fit approach (Klingenberg 2009, 2013): relative size, orientation, and position of parts may be important factors of covariation. We used here an original approach that displays the effects of independent or combined factors on the covariation patterns. We show that relative position and orientation together are mainly responsible for molar covariations in the simultaneous-fit approach (Figs. 2 and S2).

The strong interaction between m1 and m3 demonstrated here is not supported by the developmental model established on murines (Kavanagh et al. 2007) and the macroevolutionary model based on the relative size of vole molars (Renvoisé et al. 2009) and rodent molars (Labonne et al. 2012). In the early stages of molar development, molars develop sequentially, m2 initiating from m1 bud, and m3 initiating from m2 bud (Kavanagh et al. 2007; Chlastakova et al. 2011). These observations imply a stronger integration between m1 and m2 and between m2 and m3 than between m1 and m3. For vole molars, with the complete landmark scheme, the integration of M1–M3 is stronger than M2–M3 and the integration of m1–m3 is stronger than m1–m2 (Fig. 3B). These unexpectedly strong correlations seem mainly to result from covariation including relative molar orientation (Figs. 2 and S2).

The adult phenotype presents very specific patterns of integration in comparison with the expected model of early integration. After birth, tooth shape does not change except from wear (Ledevin et al. 2010), but this phenotype is highly derived, with the addition of several cusps posterior to bud subdivisions (Salazar-Ciudad and Jernvall 2002), and continuously growing molars. Integration produced by late developmental mechanisms may hide this early integration with regard to the relative size, position, and orientation of buds. Hallgrímsson et al. (2009) use the metaphor of the palimpsest to describe this subsequent wiring of components that masks prior states. Nevertheless, simplifying the description scheme may reveal early transient stages because developmental processes of tooth individuation are hierarchical (Jernvall and Thesleff 2000). Thus, taking the first three cusps to grow per molar approximates the initial arrangement of molars (their early relative size and shape).

Relevance and input of the reduced landmark scheme

On the lower row, this reduced landmark scheme confirms the strong influence of m1 on m2 and that of m2 on m3 found in a developmental study on laboratory mice (Kavanagh et al. 2007). Indeed, the best correlated molar pair on the lower row brings together m1 and m2. The m3 is slightly less correlated (Table 3; Fig. 3C) but a higher independence of this molar was expected because of differential timing and structural constraints between molars during growth. The initiation of m3 occurs perinatally in the mouse and is late in comparison with the initiation of both m1 and m2 (Chlastakova et al. 2011). A modification of the balance

between mesenchymal activation and intermolar inhibition affects the posterior molars more, because of cumulative changes along the row (Kavanagh et al. 2007). Most developmental models are based on the mouse, but some observations on the dentition of voles may confirm a slightly more independent m3. Despite aligned occlusal surfaces, the molar crowns curve in different directions. The first two molars curve toward the lingual side, while m3 curves toward the buccal side. This main pattern of covariance between molars illustrates the discrepancy of the m3 orientation (Fig. 1B). Furthermore, the lower incisor crosses from the lingual to the buccal side between m2 and m3, separating the first two molars from the third. The lower developmental and morphological integration of the last molar, m3, may result from several non-exclusive factors, such as the time-lag during molar initiation, linked to the specific cascade development of vole molars and the influence of bone and incisor root on molar position. The cumulative influence of previous molars on posterior molars may lead to the greater variability and misalignment of m3 and to the apparent developmental independence of this molar. However, on the adult phenotype (i.e., using the complete landmark scheme), this molar is highly integrated in the row at the environmental/functional level.

On the upper row, the reduced scheme analysis shows that the best correlated molar pair is M2–M3; the M1 seems more independent (Table 3; Fig. 3C). The processes and timing of development are far less studied for upper molars than for lower molars. The sequential initiation of molar buds and the inhibitory cascade model could well apply to both the lower row and the upper row, but, to our knowledge, no such studies have yet been performed. Relative integration on upper molars contrasts with that on lower molars, whatever the landmark scheme used. Several evolutionary and developmental studies have already suggested relative independence between upper and lower molar rows. The change from a typical dental morphology of one tooth class to another (i.e., homeotic changes) is independent between maxillary and mandibular teeth in many mammals (Weiss et al. 1998; Marivaux et al. 2004) and supports relative evolutionary independence. During development, the timing of M1 initiation differs from that of m1 (Schmitt et al. 1999) and they follow partially independent genetic pathways (Stock 2001; Shimizu et al. 2004; Mitsiadis and Drouin 2008). Current developmental knowledge together with our results suggest that the balance of activator and inhibitor molecules on the upper row may be different from the balance on the lower row. Whether this difference is an exception among mammals or a more general pattern is an open question.

Geometric morphometrics provides an efficient toolkit to assess modular organization, even for highly derived structures. Nonetheless, caution must be taken when considering the origin of integration. Covariation may arise at different stages, from many sources, involving complex patterns of re-wiring of traits (Hallgrímsson et al. 2009). Consequently, deciphering the origin of integration from the adult phenotype may be problematic and more superficial, with overemphasis on the very last events. Hierarchical development with an addition of complexity, together with the conservation of the individuality of parts, allows the study of early stages from adult morphology, using a description scheme that weights the relevant features at that stage. Careful attention to interesting features brought to light by developmental studies makes adult morphology relevant for the interpretation of modularity and integration patterns at both functional and developmental levels.

Acknowledgments

We thank J.-P. Quéré for the loan of the CBGP collection of common voles and two anonymous reviewers for their helpful comments on the manuscript. This work is a contribution to the BioME team of the UMR uB/CNRS 6282-Biogéosciences and to the EPHE laboratory PALEVO. This work was supported by a PhD grant to G.L. from the Région Bourgogne, and by a starting grant to N.N. (PARI-FABER 2013-0154) from the Région Bourgogne.

REFERENCES

Bookstein, F. L., Gunz, P., Mitteroecker, P., Prossinger, H., Schæfer, K., and Seidler, H. 2003. Cranial integration in *Homo*: Singular warps analysis of the midsagittal plane in ontogeny and evolution. *J. Hum. Evol.* 44: 167–187 (published online: doi: 10.1016/S0047-2484(02)00201-4).

Breuker, C. J., Debat, V., and Klingenberg, C. P. 2006. Functional evo-devo. *Trends Ecol. Evol.* 21: 488–492 (published online: doi: 10.1016/j.tree.2006.06.003).

Brunet-Lecomte, P. 1988. Les Campagnols souterrains (Terricola, Arvicolidae, Rodentia) actuels et fossiles d'Europe occidentale. Ph.D. Thesis, Burgundy University, Dijon, France.

Catón, J., and Tucker, A. S. 2009. Current knowledge of tooth development: Patterning and mineralization of the murine dentition. *J. Anat.* 214: 502–515 (published online: doi: 10.1111/j.1469-7580.2008.01014.x).

Chaline, J., Brunet-Lecomte, P., Montuire, S., Viriot, L., and Courant, F. 1999. Anatomy of the arvicoline radiation (Rodentia): Palaeogeographical, palaeoecological history and evolutionary data. *Ann. Zool. Fenn.* 36: 239–267.

Charles, C., Jaeger, J.-J., Michaux, J., and Viriot, L. 2007. Dental microwear in relation to changes in the direction of mastication during the evolution of Myodonta (Rodentia, Mammalia). *Naturwissenschaften* 94: 71–75 (published online: doi: 10.1007/s00114-006-0161-7).

Charles, C., et al. 2009. Modulation of Fgf3 dosage in mouse and men mirrors evolution of mammalian dentition. *Proc. Natl. Acad. Sci. USA* 106: 22364–22368 (published online: doi: 10.1073/pnas.0910086106).

Chlastakova, I., et al. 2011. Morphogenesis and bone integration of the mouse mandibular third molar. *Eur. J. Oral Sci.* 119: 265–274 (published online: doi: 10.1111/j.1600-0722.2011.00838.x).

Dryden, I. L., and Mardia, K. V. 1998. *Statistical Analysis of Shape*. Wiley, Chichester, UK.

Eble, G. J. 2005. Morphological modularity and macroevolution: Conceptual and empirical aspects. In W. Callebaut and and D. Rasskin-Gutman (eds.). *Modularity: Understanding the Development and Evolution of Complex Natural Systems*. The MIT Press, Cambridge, MA, pp. 221–238.

Escoufier, Y. 1973. Le traitement des variables vectorielles. *Biometrics* 29: 751–760.

Evans, A. R., Wilson, G. P., Fortelius, M., and Jernvall, J. 2007. High-level similarity of dentitions in carnivorans and rodents. *Nature* 445: 78–81 (published online: doi: 10.1038/nature05433).

Hallgrímsson, B., et al. 2009. Deciphering the palimpsest: Studying the relationship between morphological integration and phenotypic

covariation. *Evol. Biol.* 36: 355–376 (published online: doi: 10.1007/s11692-009-9076-5).
Hershkovitz, P. 1967. Dynamics of rodent molar evolution: A study based on New World Cricetinae, family Muridae. *J. Dent. Res.* 46: 829–842.
Jernvall, J., and Thesleff, I. 2000. Reiterative signaling and patterning during mammalian tooth morphogenesis. *Mech. Develop.* 92: 19–29 (published online: doi: 10.1016/S0925-4773(99)00322-6).
Jernvall, J., and Thesleff, I. 2012. Tooth shape formation and tooth renewal: Evolving with the same signals. *Development* 139: 3487–3497 (published online: doi: 10.1242/dev.085084).
Kavanagh, K. D., Evans, A. R., and Jernvall, J. 2007. Predicting evolutionary patterns of mammalian teeth from development. *Nature* 449: 427–432 (published online: doi: 10.1038/nature06153).
Kielan-Jaworowska, Z. 2004. *Mammals From the Age of Dinosaurs: Origins, Evolutions, and Structure*. Columbia University Press, New York.
Klingenberg, C. P. 2004. Integration, modules and development: Molecules to morphology to evolution. In M. Pigliucci and and K. Preston (eds.). *Phenotypic Integration: Studying the Ecology and Evolution of Complex Phenotypes*. Oxford University Press, New York, pp. 213–230.
Klingenberg, C. P. 2008. Morphological integration and developmental modularity. *Annu. Rev. Ecol. Evol. Syst.* 39: 115–132 (published online: doi: 10.1146/annurev.ecolsys.37.091305.110054).
Klingenberg, C. P. 2009. Morphometric integration and modularity in configurations of landmarks: Tools for evaluating a priori hypotheses. *Evol. Dev.* 11: 405–421 (published online: doi: 10.1111/j.1525-142X.2009.00347.x).
Klingenberg, C. P. 2013. Cranial integration and modularity: Insights into evolution and development from morphometric data. *Hystrix* 24 (published online: doi: 10.4404/hystrix-24.1-6367).
Klingenberg, C. P., and McIntyre, G. S. 1998. Geometric morphometrics of developmental instability: Analyzing patterns of fluctuating asymmetry with Procrustes methods. *Evolution* 52: 1363–1375.
Labonne, G., et al. 2012. When less means more: Evolutionary and developmental hypotheses in rodent molars. *J. Evol. Biol.* 25: 2102–2111 (published online: doi: 10.1111/j.1420-9101.2012.02587.x).
Laffont, R., Renvoisé, É., Navarro, N., Alibert, P., and Montuire, S. 2009. Morphological modularity and assessment of developmental processes within the vole dental row (*Microtus arvalis*, Arvicolinae, Rodentia). *Evol. Dev.* 11: 302–311 (published online: doi: 10.1111/j.1525-142X.2009.00332.x).
Ledevin, R., Quéré, J.-P., and Renaud, S. 2010. Morphometrics as an insight into processes beyond tooth shape variation in a bank vole population. *PLoS ONE* 5: e15470 (published online: doi: 10.1371/journal.pone.0015470).
Luo, Z. X., Cifelli, R. L., and Kielan-Jaworowska, Z. 2001. Dual origin of tribosphenic mammals. *Nature* 409: 53–57 (published online: doi: 10.1038/35051023).
Marivaux, L., Vianey-Liaud, M., and Jaeger, J.-J. 2004. High-level phylogeny of early Tertiary rodents: Dental evidence. *Zool. J. Linn. Soc.* 142: 105–134 (published online: doi: 10.1111/j.1096-3642.2004.00131.x).
Mitsiadis, T. A., and Drouin, J. 2008. Deletion of the Pitx1 genomic locus affects mandibular tooth morphogenesis and expression of the *Barx1* and *Tbx1*genes. *Dev. Biol.* 313: 887–896 (published online: doi: 10.1016/j.ydbio.2007.10.055).
Mitteroecker, P., and Bookstein, F. 2007. The conceptual and statistical relationship between modularity and morphological integration. *Syst. Biol.* 56: 818–836 (published online: doi: 10.1080/10635150701648029).
Olson, E. C., and Miller, R. L. 1958. *Morphological Integration*. University of Chicago Press, Chicago, IL.
Palmer, A. R., and Strobeck, C. 1986. Fluctuating asymmetry: Measurement, analysis, patterns. *Ann. Rev. Ecol. Syst.* 17: 391–421 (published online: doi: 10.1146/annurev.es.17.110186.002135).
Polly, P. D. 2007. Development with a bite. *Nature* 449: 413–415 (published online: doi: 10.1038/449413a).
Polly, P. D. 2012. Movement adds bite to the evolutionary morphology of mammalian teeth. *BMC Biol.* 10: 69 (published online: doi: 10.1186/1741-7007-10-69).
R Development Core Team. 2011. *R: A Language and Environment for Statistical Computing*. R Foundation for Statistical Computing, Vienna, Austria.
Reisz, R. R. 2006. Origin of dental occlusion in tetrapods: Signal for terrestrial vertebrate evolution? *J. Exp. Zool. (Mol. Dev. Evol.)* 306B: 261–277 (published online: doi: 10.1002/jez.b.21115).
Renaud, S., Pantalacci, S., Quéré, J.-P., Laudet, V., and Auffray, J.-C. 2009. Developmental constraints revealed by co-variation within and among molar rows in two murine rodents. *Evol. Dev.* 11: 590–602 (published online: doi: 10.1111/j.1525-142X.2009.00365.x).
Renvoisé, É., Evans, A. R., Jebrane, A., Labruère, C., Laffont, R., and Montuire, S. 2009. Evolution of mammal tooth patterns: New insights from a developmental prediction model. *Evolution* 63: 1327–1340 (published online: doi: 10.1111/j.1558-5646.2009.00639.x).
Renvoisé, É., et al. 2012. Microevolutionary relationships between phylogeographical history, climate change and morphological variability in the common vole (*Microtus arvalis*) across France. *J. Biogeogr.* 39: 698–712 (published online: doi: 10.1111/j.1365-2699.2011.02611.x).
Rohlf, F. J., and Corti, M. 2000. Use of two-block partial least-squares to study covariation in shape. *Syst. Biol.* 49: 740–753 (published online: doi: 10.1080/106351500750049806).
Salazar-Ciudad, I., and Jernvall, J. 2002. A gene network model accounting for development and evolution of mammalian teeth. *Proc. Natl. Acad. Sci. USA* 99: 8116–8120 (published online: doi: 10.1073/pnas.132069499).
Satoh, K. 1997. Comparative functional morphology of mandibular forward movement during mastication of two murid rodents, *Apodemus speciosus* (Murinae) and *Clethrionomys rufocanus* (Arvicolinae). *J. Morphol.* 231: 131–142.
Schmitt, R., Lesot, H., Vonesch, J.-L., and Ruch, J.-V. 1999. Mouse odontogenesis in vitro: The cap-stage mesenchyme controls individual molar crown morphogenesis. *Int. J. Dev. Biol.* 43: 255–260.
Shimizu, T., Oikawa, H., Han, J., Kurose, E., and Maeda, T. 2004. Genetic analysis of crown size in the first molars using SMXA recombinant inbred mouse strains. *J. Dent. Res.* 83: 45–49 (published online: doi: 10.1177/154405910408300109).
Smits, P. D., and Evans, A. R. 2012. Functional constraints on tooth morphology in carnivorous mammals. *BMC Evol. Biol.* 12: 146 (published online: doi: 10.1186/1471-2148-12-146).
Stehlin, H. G., and Schaub, S. 1951. Die trigonodontie der simplicidentaten Nager. *Schweiz. Paläont. Abh.* 67: 1–385.
Stock, D. W. 2001. The genetic basis of modularity in the development and evolution of the vertebrate dentition. *Philos. Trans. R. Soc. Lond. B* 356: 1633–1653 (published online: doi: 10.1098/rstb.2001.0917).
Streissguth, A. P., Bookstein, F. L., Sampson, P. D., and Barr, H. M. 1993. *The Enduring Effects of Prenatal Alcohol Exposure on Child Development: Birth Through Seven Years, a Partial Least Squares Solution*. The University of Michigan Press, Ann Arbor, MI.
Van der Meulen, A. J. 1973. Middle Pleistocene small mammals from the Monte Peglia (Orvieto, Italy) with special reference to the phylogeny of *Microtus* (Arvicolidae, Rodentia). *Quaternaria* 16: 1–144.
Van Valen, L. 1974. Multivariate structural statistics in natural history. *J. Theoret. Biol.* 45: 235–247.
Van Valen, L. 2005. The statistics of variation. In B. Hallgrímsson and and B. K. Hall (eds.). *Variation: A Central Concept in Biology*. Elsevier Academic Press, Boston, MA, pp. 29–48.
Vorontsov, N. N. 1979. *Evolution of the Alimentary System in Myomorph Rodents*. Smithsonian Institution and the National Science Foundation, Washington, DC.
Wagner, G. P. 1996. Homologues, natural kinds and the evolution of modularity. *Am. Zool.* 36: 36–43 (published online: doi: 10.1093/icb/36.1.36).
Weiss, K. M., Stock, D. W., and Zhao, Z. 1998. Dynamic interactions and the evolutionary genetics of dental patterning. *Crit. Rev. Oral Biol. Med.* 9: 369–398 (published online: doi: 10.1177/10454411980090040101).

SUPPORTING INFORMATION

Additional supporting information may be found in the online version of this article at the publisher's web-site.

Fig. S1. The occlusal surface of upper molars (M1, M2, M3) and lower molars (m1, m2, m3) of *Microtus arvalis* are represented. The first three cusps to grow and to evolve are called protocone (Pr), paracone (Pa), and metacone (Me) on upper molars, and protoconid (Prd), metaconid (Med), and entoconid (End) on lower molars. Before the measurement of landmarks, M1 is oriented on A–B axis, M2 on C–D axis, M3 on E–F axis, m1 on G–H axis, m2 on I–J axis, and m3 on K–L axis. Thirty-eight landmarks on upper molars and 47 on lower molars are used for morphometrics. The samples were from Espezel (Aude, $n = 48$), Versailles (Yvelines, $n = 36$), Parc de la Vanoise (Savoie, $n = 34$), Vittel (Vosges, $n = 32$), and St Michel en l'Herm (Vendée, $n = 32$).

Fig. S2. Comparison of influential factors in simultaneous and separate Procrustes approaches using variance–covariance (VCV) matrices scaled by variances. The influence on the pattern of covariation of relative sizes, orientations and positions of molars was presented here for variation among-individuals (VarInd) of the lower row (A), for fluctuating asymmetry (FA) on upper row (B), and for IndVar on upper row (C).

Table S1. Results of the MANCOVA. Size and population origin are significant for each level at which modularity analysis would be assessed.

Table S2. Procrustes ANOVA results on upper and lower rows after simultaneous Procrustes fit or separate Procrustes fit.